Journal of Alloys and Compounds 509 (2011) 9015–9018

Contents lists available at ScienceDirect

Journal of Alloys and Compounds

journal homepage: www.elsevier.com/locate/jallcom

Effect of solubility on strengthening of Ag–Cu ultrafine eutectic composites

E.M. Park[a], G.A. Song[a], J.K. Lee[b], M.H. Lee[c], H.S. Lee[c], J.Y. Park[a], N.S. Lee[a], Y. Seo[a], K.B. Kim[a,*]

[a] Faculty of Nanotechnology and Advanced Materials Engineering, Sejong University, Gunja-dong, Gwangjin-gu, Seoul 143-747, Republic of Korea
[b] Division of Advanced Materials Engineering, Kongju National University, Chenan 331-717, Republic of Korea
[c] Production Technology R&D Division, Korea Institute of Industrial Technology, 7-47 Songdo-Dong, Yeonsu-Gu, Incheon 406-840, Republic of Korea

ARTICLE INFO

Article history:
Received 7 April 2011
Received in revised form 1 June 2011
Accepted 6 June 2011
Available online 29 June 2011

Keywords:
Nanostructured materials
Rapid-solidification
Mechanical properties
Scanning electron microscopy

ABSTRACT

A series of binary $Ag_{80-x}Cu_{20+x}$ ultrafine eutectic composites with $x = 0$, 10, 20, 30 and 40 is prepared by copper mold casting in order to systematically investigate an influence of asymmetrical solubility between Ag and Cu solid solutions on the strengthening of ultrafine eutectic composites. The asymmetrical solubility of the ultrafine eutectic composites determined by the effective solubility index derived from rule of mixtures plays an important role to maintain the strength even with increasing the volume fraction of the micron-scale dendrites. Based on the results, the control of the strengthening of the ultrafine eutectic composites is governed by not only well-known volume fraction of the micron-scale dendrites but also the solubility in the micron-scale dendrites.

1. Introduction

Bulk metallic glasses (BMGs) and nano/ultrafine-grained metallic materials have received much attention due to their unique physical properties, i.e. high strength compared with conventional coarse-grained metallic materials [1,2]. However, the final fracture of the BMGs and nano/ultrafine-grained metallic materials often happens catastrophically and involves very little macroscopic plastic deformation due to highly localized shear bands [3]. Recently, a series of ultrafine eutectic composites has been successfully developed in Ti-[4,5], Zr-[6,7] and Mg-[8] based alloy systems. These unique composites exhibit promising high strength combined with superior plastic deformability at room temperature. The detailed investigation of the deformation mechanisms points out that the micron-scale dendrite has a strong influence to control the plasticity whereas the ultrafine eutectic matrix can be effective to back up the strength of the sample [3,9–13]. Based on these results, it is possible to understand that the harmonic combination of the size difference between the micron- scale dendrites and ultrafine eutectic matrix i.e. length-scale heterogeneity can result in both high strength and large plasticity of the samples.

Along the line to demonstrate the influence of the length-scale heterogeneity on the mechanical properties of the ultrafine eutectic alloys, several trials have been performed in Ti- [4,14] and Al- [15,16] based alloys by adding the minor elements possibly causing the variation of the lamellar spacing during the growth of the eutectic colony. Such approach to control the microstructural heterogeneities is very useful to form the bimodal ultrafine eutectic structure containing the different eutectic phases with the length-scale heterogeneity so called a mixture of the coarse and fine eutectic colonies [12]. Furthermore, the detailed chemical analysis of Ti-based bimodal eutectic alloys indicates the existence of the chemical heterogeneity in the constituent phases [17]. For example, it is clear to demonstrate a high amount of Sn solute not in TiFe intermetallics but in β-Ti solid solution.

On the other hand, there are some reports on enhancement of both strength and plasticity in the solid solution β-Ti alloy by controlling the solutes even without the formation of the ultrafine eutectic matrix [18]. This implies that the local structural change/clustering in the solid solution β-Ti phase can occur via dynamic transformation along the grain boundary [19]. Hence, it is feasible to suggest that a selection of the solute and solubility in the micron-scale dendrites of the ultrafine eutectic composites can be one of the crucial factors to control further enhanced mechanical properties. However, so far there is no trial to understand the effect of the solutes in the micron-scale dendrites on the microstructure and mechanical properties of the ultrafine eutectic composites.

In this investigation, a series of binary $Ag_{80-x}Cu_{20+x}$ alloys with $x = 0$, 10, 20, 30 and 40 at.% has been chosen to elucidate the influence of the solutes on the microstructure and mechanical properties of the ultrafine eutectic composites. Since the binary Ag–Cu alloys consist of only a mixture of solid solution phases having the asymmetrical solubility between the Ag and Cu solid solutions [20], it is possible to systematically compare the effect

* Corresponding author. Tel.: +82 2 3408 3690; fax: +82 2 3408 3664.
E-mail address: kbkim@sejong.ac.kr (K.B. Kim).

0925-8388/$ – see front matter © 2011 Elsevier B.V. All rights reserved.
doi:10.1016/j.jallcom.2011.06.021

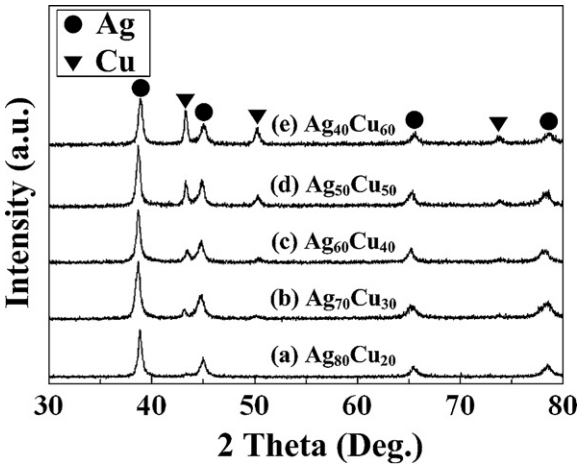

Fig. 1. XRD patterns obtained from the as-cast $Ag_{80-x}Cu_{20+x}$ alloys with $x = 0$, 10, 20, 30 and 40.

of the solutes on the strengthening of the ultrafine eutectic composites combined with a variation of the volume fraction of the micron-scale dendrites.

2. Experimental

A series of $Ag_{80-x}Cu_{20+x}$ ($x = 0$, 10, 20, 30 and 40 at.%) alloys were prepared by induction melting of pure elements under argon atmosphere and directly casted into cylindrical rods shape with 3 mm diameter and 50 mm length using an injection casting facility. The microstructures of as-cast sample were examined using scanning electron microscopy (SEM) (Jeol, JSM-6390). The volume fraction of the primary dendrites and matrix were determined by two different method, i.e. SEM image analysis and lever rule with equilibrium binary phase diagram [20]. The phase analysis was performed using an energy-dispersive X-ray spectrometer (EDS, Kevex superdry) attached to the scanning electron microscope and X-ray diffraction (XRD) (Rigaku RINT2000, monochromatic Cu Kα radiation). Transmission electron microscopy (TEM: JEM 2010) was used for a structural characterization. Thin foils for TEM were prepared by conventional ion milling (Gatan, Model 600). The room temperature mechanical properties were evaluated by uniaxial compression tests with 2:1 aspect ratio cylindrical specimens under loading at an initial strain rate of $1 \times 10^{-3}\ s^{-1}$.

3. Results

Fig. 1 shows XRD patterns of as-cast $Ag_{80-x}Cu_{20+x}$ alloys with $x = 0$, 10, 20, 30 and 40. The diffraction peaks in Fig. 1[(a)–(e)] are identified as a mixture of face-centered cubic (fcc) Ag and Cu solid solutions having same crystalline symmetry, ($Fm\bar{3}m$). With decreasing Ag content, the diffraction intensity of the Cu solid solution gradually increases whereas that of Ag slightly decreases, indicating an increase of the volume fraction of Cu solid solution.

Fig. 2[(a)–(e)] displays SEM images of the as-cast $Ag_{80-x}Cu_{20+x}$ alloys with $x = 0$, 10, 20, 30 and 40. Backscattered electron (BSE) micrographs in Fig. 2(a) shows that the $Ag_{80}Cu_{20}$ alloy consists of the micro-scale primary Ag dendrites homogeneously distributed in the matrix. The volume fraction of the primary Ag dendrites can be measured to be about 87.5 vol.%. Furthermore, the morphology of the primary Ag dendrites is quire coarse and continuous indicating that the active growth of the Ag dendrites upon solidification. When the content of Ag is 70 at.% as shown in Fig. 2(b), the volume fraction of the primary Ag dendrites slightly decreases down to 67.7 vol.% with rather sharp morphology. Interestingly, one can find that the volume fraction of the Ag dendrites for the $Ag_{80}Cu_{20}$ and $Ag_{70}Cu_{30}$ alloys measured by a well-known lever rule [21] to be about 75.4 vol.% and 40.9 vol.%, respectively is considerably different to that measured by the SEM shown in Fig. 2(a) and (b). Furthermore, the EDX analysis from Fig. 2(b) indicates that the Ag dendrite contains 16.44 ± 3.69 at.% of solute Cu.

The SEM image in Fig. 2(c) from the as-cast $Ag_{60}Cu_{40}$ alloy with an eutectic composition reveals that no contrast difference is visible throughout the sample possibly due to the limit resolution of the SEM in the present study. The detailed microstructure of this alloy will be shown in Fig. 3 using TEM. Fig. 2(d) shows the secondary electron micrograph of the $Ag_{50}Cu_{50}$ alloy consisting of primary Cu dendrites uniformly dispersed in the matrix. The volume fraction of the micro-scale Cu dendrites is measured to be about 20.0 vol.%. The EDX analysis of the Cu dendrite in Fig. 2(d) reveals that the Cu dendrite contains 7.5 ± 3.21 at.% of the solute Ag. As the Ag content decreases down to 40 at.%, i.e. $Ag_{40}Cu_{60}$, the volume fraction of the primary Cu dendrites continuously increases up to 46.1 vol.% as shown in Fig. 2(e). Furthermore, there is a significant growth of the micro-scale Cu dendrites upon solidification. One can find that the volume fraction estimated by the lever rule is well consistent to that measured by SEM as shown in Fig. 2(d) and (e). By comparing the Ag dendrite-containing i.e. $Ag_{80}Cu_{20}$ and $Ag_{70}Cu_{30}$ and Cu dendrite-containing, i.e. $Ag_{50}Cu_{50}$ and $Ag_{40}Cu_{60}$ alloys, it is possible to suggest that the solubility of Cu in the Ag dendrites can be much higher than the solubility of Ag in the Cu dendrites and thus cause the different morphology of the dendrites upon solidification. The Table 1 shows a summary of the phase identification and volume fraction of the micron-scale dendrites based on both experimental measurement and theoretical lever rule calculation from the a binary phase diagram. Hence, it is clear to demonstrate that the asymmetrical solubility between the constituent elements has a strong influence to control the morphology and volume fraction of the micron-scale dendrites upon solidification.

Fig. 3 shows a TEM bright-field image (a) and a corresponding selected area diffraction pattern (b) of the as-cast $Ag_{60}Cu_{40}$ binary alloy. The TEM image displays the formation of fine lamellar structure with an inter-layer spacing of 43–50 nm. The selected area diffraction pattern (SADP) in Fig. 3(b) obtained from the area indicated by dashed square in Fig. 3(a) corresponds to the [1 1 2] zone axis of the Ag and Cu solid solutions, respectively. Furthermore, it is worth to note that typical double diffraction spots appear as indicated in Fig. 3(b) implying the structural coherency between Ag and Cu solid solutions. The EDX analysis in the TEM exhibits that the Cu solid solution, i.e. the fine layer indicated by arrows contains 5.26 ± 2.82 at.% of the Ag solute whereas the Ag solid solution, i.e. the coarse layer contains 18.43 ± 2.98 at.% of the Cu solute indicating the asymmetrical solubility between Ag and Cu solid solutions as similarly demonstrated from SEM shown in Fig. 2(a)–(e). Therefore, it is believed that such asymmetrical solubility can occur not only in the ultrafine eutectic matrix but also in the micron-scale dendrites of the ultrafine eutectic composites.

In order to evaluate the mechanical properties of a series of as-cast $Ag_{80-x}Cu_{20+x}$ ultrafine eutectic composites with $x = 0$, 10, 20, 30 and 40 the room temperature compression tests were carried out at a strain rate of $1 \times 10^{-3}\ s^{-1}$. Fig. 4 shows the compressive stress–strain curves of the as-cast $Ag_{80-x}Cu_{20+x}$ ultrafine eutectic composites with $x = 0$, 10, 20, 30 and 40. All specimens undergo considerable plastic strain without fracture implying the occurrence of the homogeneous deformation. One can find that the $Ag_{60}Cu_{40}$ alloy consisting of ultrafine eutectic structure without the micron-scale primary dendrites exhibits the highest compressive yield strength of $\sigma_y = 430$ MPa. In contrast, the ultrafine eutectic alloys containing the micron-scale Ag dendrites, i.e. $Ag_{80}Cu_{20}$ and $Ag_{70}Cu_{30}$ alloys exhibit a tendency of the decrease of the yield strength down to 128 MPa with increasing Ag content. Similarly, the yield strength of the samples containing the micron-scale Cu dendrites, i.e. the $Ag_{50}Cu_{50}$ and $Ag_{40}Cu_{60}$ alloys decreases gradually.

Fig. 5 indicates the yield strength of a series of as-cast $Ag_{80-x}Cu_{20+x}$ ultrafine eutectic composites with $x = 0$, 10, 20, 30 and

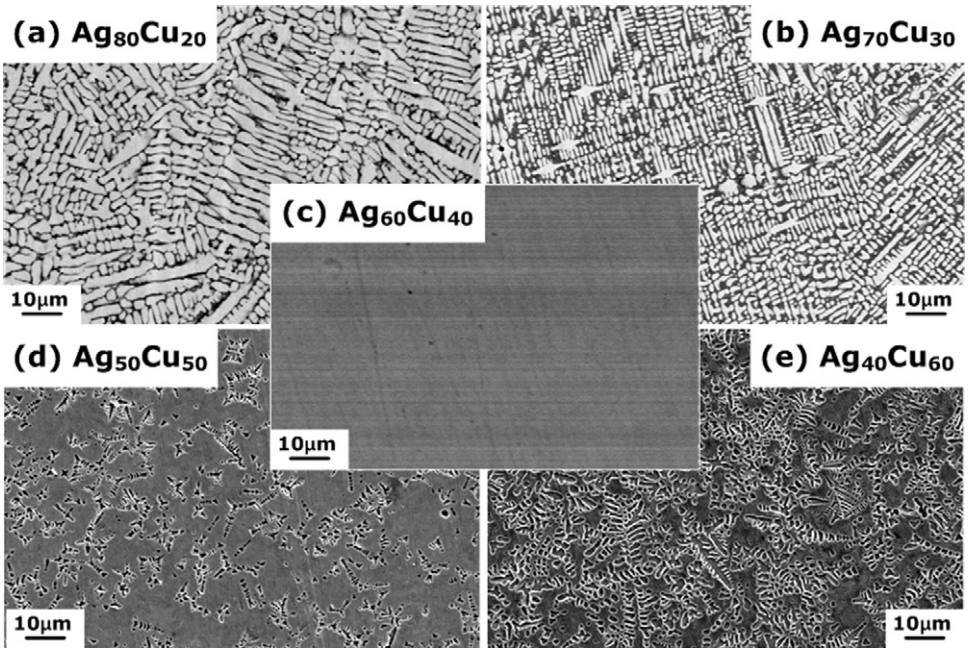

Fig. 2. Backscattered electron SEM micrographs of the $Ag_{80-x}Cu_{20+x}$ alloys ($x = 0$, 10 and 20): (a) $x = 0$, (b) $x = 10$ and (c) $x = 20$. SEM secondary electron images of the $Ag_{80-x}Cu_{20+x}$ alloys ($x = 30$ and 40): (d) $x = 30$ and (e) $x = 40$.

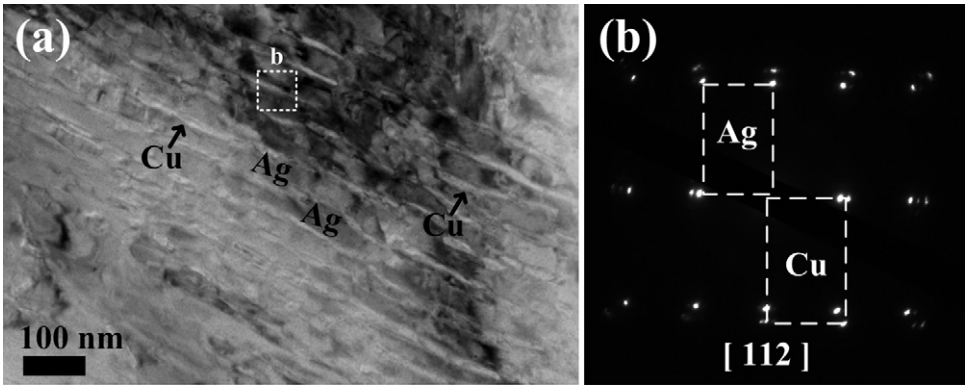

Fig. 3. Bright field TEM image (a) and corresponding selected area diffraction pattern (b) of the as-cast $Ag_{60}Cu_{40}$ alloy.

40 as a function of the volume fraction of the micron-scale Ag or Cu dendrites embedded on the ultrafine eutectic matrix. As shown in Fig. 4, there is a general tendency to decrease the strength of the samples with increasing the volume fraction of the micron-scale Ag or Cu dendrites. However, the decrease of the yield strength of the micron-scale Ag dendrite-containing ultrafine eutectic composites is less sensitive compared to that of the micron-scale Cu dendrite-containing ultrafine eutectic composites possibly due to the symmetrical solubility.

In the present investigation, it is interesting to point out that the $Ag_{60}Cu_{40}$ ultrafine eutectic alloy consisting of a mixture of Ag and Cu solid solution phases presents quite high yield strength of 430 MPa. Considering rule of mixtures between Ag and Cu with the yield strength of 15 and 48 [22] MPa, respectively, it is feasible to suggest that the incredible increase of the yield strength of the $Ag_{60}Cu_{40}$ ultrafine eutectic alloy can occur due to the effects from both the solid-solution strengthening of Ag and Cu phases and introduction of the interfaces at the lamellar eutectic structure.

Table 1
Comparison between the experimental volume fraction of dendrite (V_e) and theoretical volume fraction of dendrite by lever rule (V_T) of Ag–Cu alloys.

Composition (at.%)	Phases	V_e (%)	V_T(%)
$Ag_{80}Cu_{20}$	Primary dendrite (Ag solid solution) Eutectic matrix (Ag + Cu solid solutions)	87.5	75.4
$Ag_{70}Cu_{30}$	Primary dendrite (Ag solid solution) Eutectic matrix (Ag + Cu solid solutions)	67.7	40.9
$Ag_{60}Cu_{4O}$	Eutectic matrix (Ag + Cu solid solutions)	0	0
$Ag_{50}Cu_{50}$	Primary dendrite (Cu solid solution) Eutectic matrix (Ag + Cu solid solutions)	20.0	18.9
$Ag_{40}Cu_{60}$	Primary dendrite (Cu solid solution) Eutectic matrix (Ag + Cu solid solutions)	46.1	36.7

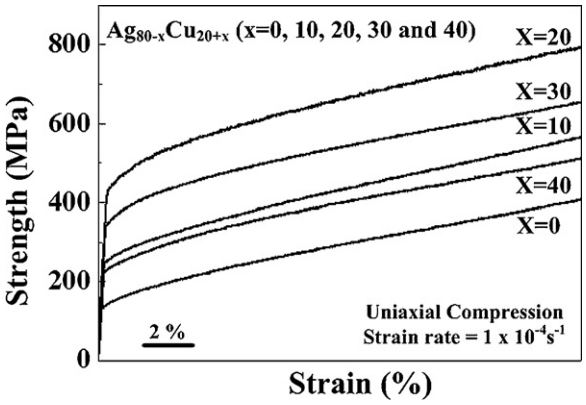

Fig. 4. Compressive stress-strain curves of the $Ag_{80-x}Cu_{20+x}$ alloys with $x = 0, 10, 20, 30$ and 40 at room temperature compression.

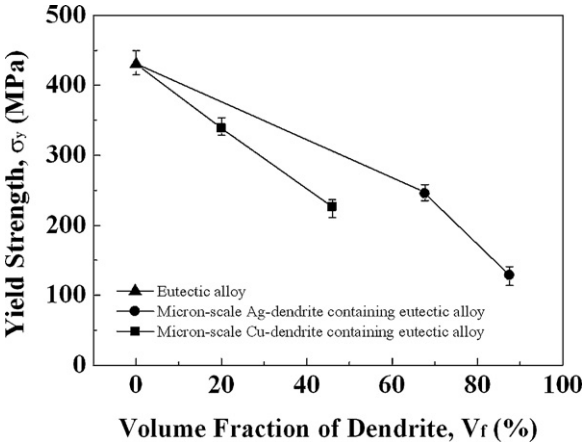

Fig. 5. Yield strength (σ_y) obtained compressive tests as a function of the volume fraction of the Ag or Cu solid solution dendrite (V_f) of the $Ag_{80-x}Cu_{20+x}$ alloys with $x = 0, 10, 20, 30$ and 40.

As a first step to understand the effect of the solid-solution strengthening, the yield strength of the ultrafine eutectic composites can be as in below;

$$\sigma_{comp} = A_s(V_d\sigma_d + V_e\sigma_e)$$

where σ_{comp} is the value of the yield strength, V_d and V_e are the volume fractions of the dendrites and ultrafine eutectic matrix, σ_d and σ_e are yield strength of the pure elements and fully eutectic alloy and A_s refers to the effective solubility index. This can apply when there is no interaction between the matrix and dendrite phase which is continuous, uniform, unidirectional and is gripped firmly by the matrix without slipping at the interface. The effective solubility index of the micron-scale Ag dendrite-containing ultrafine eutectic composite is 1.79 whereas that of the ultrafine eutectic composites containing the micron-scale Cu dendrites is 0.93. This is also in good agreement with the EDX analysis showing that the Ag dendrites contain higher concentration of the Cu solute, i.e. 16 at.% than the Cu dendrites with Ag solutes of about 7 at.% as described in Figs. 2 and 3. Hence, it is possible to conclude that the solubility of the phase in the ultrafine eutectic composites can be treated as one of the important parameters to control the strength of the samples.

4. Summary

A series of $Ag_{80-x}Cu_{20+x}$ ultrafine eutectic composites with $x = 0$, 10, 20, 30 and 40 has been successfully fabricated varying the volume fraction of the micron-scale dendrites and ultrafine eutectic matrix. Among them, an $Ag_{60}Cu_{40}$ ultrafine eutectic alloy exhibits the highest yield strength of 430 MPa whereas the ultrafine eutectic composites containing the micron-scale Ag or Cu dendrites embedded on the ultrafine eutectic matrix reveal a significant decrease of the strength down to 128 MPa. However, the detailed investigation of these alloys indicates that the decrease of the strength has a strong dependence on the solubility in the solid solution phase. The alloys with the micron-scale Ag dendrites having the large solubility of Cu is less sensitive to those with the micron-scale Cu dendrites having the small solubility of Ag even though these alloys have more or less identical volume fraction of the micron-scale dendrites. Furthermore, such asymmetrical solubility between Ag and Cu solid solution can be identified using the effective solute index. Therefore, it is feasible to suggest that the strengthening of the Ag–Cu ultrafine eutectic composites is depending on not only the volume fraction of the micron-scale dendrites but also the solubility in the solid solution phases.

Acknowledgements

This work was supported by the Ministry of Knowledge Economy (MKE) and Korea Institute of Technology Evaluation and Planning (KETEP) and National Research Foundation of Korea (NRF) grant funded by the Korea government (MEST) of Korea Ministry of Education, Science and Technology. (no. 2010-0013854).

References

[1] H. Gleiter, Acta Mater. 48 (2000) 1–29.
[2] W.L. Johnson, MRS Bull. 24 (1999) 42–56.
[3] J.M. Park, K.B. Kim, W.T. Kim, D.H. Kim, Appl. Phys. Lett. 91 (2007) 131907.
[4] J.H. Han, K.B. Kim, S. Yi, J.M. Park, S.W. Sohn, T.E. Kim, D.H. Kim, J. Das, J. Eckert, Appl. Phys. Lett. 93 (2008) 141901.
[5] D.V. Louzguine, H. Kato, L.V. Louzguina, A. Inoue, J. Mater. Res. 19 (2004) 3600–3606.
[6] U. Kühn, J. Eckert, N. Mattern, L. Schultz, Mater. Sci. Eng. A-Struct. 375–377 (2004) 322–326.
[7] J. Das, W. Löser, U. Kühn, J. Eckert, S. Roy, L. Schultz, Appl. Phys. Lett. 82 (2003) 4690.
[8] G.A. Song, W.H. Lee, N.S. Lee, J.M. Park, D.H. Kim, J.S. Lee, J.S. Park, K.B. Kim, J. Mater. Res. 24 (2009) 2892–2898.
[9] K.B. Kim, J. Das, W. Xu, Z.F. Zhang, J. Eckert, Acta Mater. 54 (2006) 3701–3711.
[10] D.V. Louzguine, L.V. Louzguina, H. Kato, A. Inoue, Acta Mater. 53 (2005) 2009–2017.
[11] J.M. Park, S.W. Sohn, D.H. Kim, K.B. Kim, W.T. Kim, J. Eckert, Appl. Mater. Lett. 92 (2008) 091910.
[12] J. Das, K.B. Kim, F. Baier, W. Löser, J. Eckert, Appl. Phys. Lett. 87 (2005) 161907.
[13] K.B. Kim, J. Das, F. Baier, J. Eckert, J. Alloys Compd. 434–435 (2007) 106–109.
[14] J.H. Han, K.B. Kim, S. Yi, J.M. Park, D.H. Kim, S. Pauly, J. Eckert, Appl. Phys. Lett. 93 (2008) 201906.
[15] J.M. Park, N. Mattern, U. Kühn, J. Eckert, K.B. Kim, W.T. Kim, K. Chattopadhyay, D.H. Kim, J. Mater. Res. 24 (2009) 2605–2609.
[16] J.M. Park, K.B. Kim, D.H. Kim, N. Mattern, R. Li, G. Liu, J. Eckert, Intermetallics 18 (2010) 1829–1833.
[17] G.A. Song, J.H. Han, T.E. Kim, J.M. Park, D.H. Kim, S. Yi, Y. Seo, N.S. Lee, K.B. Kim, Intermetallics 19 (2011) 536–540.
[18] X.F. Zhang, K.B. Kim, S. Yi, Intermetallics 18 (2010) 725–729.
[19] K.B. Kim, X.F. Zhang, S. Yi, J. Phys. D: Appl. Phys. 42 (2009) 032002.
[20] T.B. Massalski, Binary Alloy Phase Diagram , ASM International, West Cohshohocken, PA, 1990.
[21] D.A Porter, K.E. Easterling, Phase Transformation on Metals and Alloys , 1992, Chapter.1.
[22] ASM Handbook 08, Mechanical Testing & Evaluation.